All inhibitors were tested from 0.1 to 10 μM and viability was monitored by trypan blue exclusion. The final concentrations of HA used to inhibit tyrosine kinases in this study were approximately 1/10 to 1/20 of that required for direct inhibition of Ca^{2+} entry into T cells.

17. Cells were incubated for 48 hours in IL-2–free culture medium containing 0.5% serum. Cell viability was >95%. Inhibitor-pretreated or untreated lymphocytes were then stimulated with RANTES for 30 s to 5 min, rapidly separated by centrifugation at 4°C, and lysed for 15 min on ice with periodic mixing in lysis buffer [1% Triton X-100, 20 mM tris-HCl (pH 8.0), 137 mM NaCl, 15% glycerol, 5 mM EDTA] containing phosphatase and protease inhibitors [1 mM phenylmethylsulfonyl fluoride, aprotinin (10 μg/ml), leupeptin (10 μg/ml), 1 mM sodium orthovanadate, 1 mM EGTA, 100 μM β-glycerophosphate]. The lysates were analyzed under reducing conditions on 10% SDS-polyacrylamide gels (Novex). Resolved proteins were transferred to activated Immobilon P membranes (Millipore) for immunoblot analysis. Membranes were incubated first in tris-buffered saline (TBS) containing 5% BSA, 0.1% Tween-20, and 0.05% thimerosol and then overnight with antibodies (4G10) to phosphotyrosine (1 μg/ml) (UBI). The filters were then washed extensively (TBS containing 0.5% NP-40), incubated with secondary horseradish peroxidase–coupled antibodies to mouse immunoglobulin (Amersham), washed again, incubated with ECL reagent (Amersham), and exposed to BIOMAX-MR film (Eastman Kodak).
18. Cloning studies, with primers targeted to homologous domains of the chemokine 7TM receptor family, have identified a potentially uncharacterized receptor in the T cell clone and peripheral blood lymphocytes.
19. N. J. Skelton, F. Aspiras, T. Schall, *Biochemistry* **34**, 5329 (1995); K. Rajarathnum *et al.*, *Science* **264**, 90 (1994); G. J. Graham *et al.*, *J. Biol. Chem.* **269**, 4974 (1994).
20. L. M. C. Webb, M. U. Ehrengruber, I. Clark-Lewis, M. Baggiolini, A. Rot, *Proc. Natl. Acad. Sci. U.S.A.* **90**, 7158 (1993); D. P. Witt and A. D. Lander, *Curr. Biol.* **4**, 394 (1994); Y. Tanaka *et al.*, *Nature* **361**, 79 (1993).
21. K. B. Bacon, R. D. Camp, F. M. Cunningham, P. M. Woollard, *Br. J. Pharmacol.* **95**, 966 (1988).
22. Fluorescence-activated cell sorting (FACS) was performed according to standard methods. Quiescent lymphocytes were left unstimulated or were stimulated for 48 hours with RANTES (1 μM), washed in phosphate-buffered saline containing 0.05% NaN_3 and 1% BSA, incubated at a concentration of 2×10^5 cells per well in a 96-well conical plate (Costar Serocluster) with fluorescein isothiocyanate–coupled antibodies to human CD25 (IL-2R) (Becton Dickinson) for 30 min, washed three times, and then analyzed with a Becton Dickinson FACScan. It was necessary to render the cells quiescent before FACS analysis because the cells are maintained in IL-2–containing medium; thus, the level of IL-2 receptor expression is high and small changes are masked.
23. Enzyme-linked immunosorbent assay measurements were made according to standard protocols with quiescent T cells, in order to avoid the high basal expression of cytokines such as IL-2, IL-5, and IL-4. Antibodies [anti–IL-5 (39D10), rat immunoglobulin (Ig) G2a; anti–IL-4 (8D4-8), mouse IgG1; anti–interferon γ (A35), mouse IgG1; anti–IL-2 (BG-5), mouse IgG1] (DNAX) were coated onto the wells of a 96-well polyvinyl chloride plate and incubated for 2 hours at 37°C. After washing the wells, the samples were incubated with the coating antibody for 2 hours at room temperature, after which the wells were washed and incubated for 1 hour at room temperature with nitroiodophenylacetate-coupled secondary antibodies (50 μg/ml) [anti–IL-5 (5A10), rat IgG2a; anti–IL-4 (MP4-25D2), rat IgG1; anti–interferon γ (B27), mouse IgG1; anti–IL-2, goat polyclonal] (DNAX). Immune complexes were revealed by incubation with tertiary horseradish peroxidase–coupled antibodies to nitroiodophenylacetate for 1 hour at room temperature. After incubation, ABTS solution was added and absorbance at 405 to 600 nm measured after the color had developed. Results were analyzed with SoftMax software (Molecular Devices) to obtain absolute protein values.
24. We thank H. Yssel (DNAX) for the initial provision of the T cell clone. B.A.P. was supported by NIH fellowship GM07065. B.A.P. and P.G. were also supported by American Cancer Society grant DB-26E. DNAX Research Institute is supported by Schering Plough.

27 April 1995; accepted 18 July 1995

Regulation of Hippocampal Transmitter Release During Development and Long-Term Potentiation

Vadim Y. Bolshakov and Steven A. Siegelbaum

Developmental changes in rat hippocampal transmitter release and synaptic plasticity were investigated. Recordings from pairs of pyramidal neurons in slices showed that an action potential in a CA3 neuron released only a single quantum of transmitter onto a CA1 neuron. Failures of synaptic transmission reflected probabilistic transmitter release. The probability of release (P_r) was 0.9 in 4- to 8-day-old rats and decreased to less than 0.5 at 2 to 3 weeks. Long-term potentiation (LTP) in 2- to 3-week-old rats was associated with an increase in P_r from a single synaptic site. The high initial P_r in 4- to 8-day-old rats normally occludes the expression of LTP at this stage.

Long-term potentiation (LTP) (*1*) and long-term depression (LTD) (*2*) of hippocampal synaptic transmission are opposing forms of activity-dependent plasticity that may underlie learning and memory and the fine tuning of synaptic connections during development (*3*). The expression of hippocampal LTP and LTD in rats changes markedly during the first 3 weeks after birth, a critical period in the establishment of synaptic connections (*4*). Whereas LTP is observed only in rats that are >2 weeks old (*5*, *6*), LTD is most prominent during the first 10 days after birth (*6*, *7*). This complementary pattern of expression of LTP and LTD is likely important for the formation of the normal pattern of synaptic connections and early learning and memory. However, controversy surrounds the basic properties of synaptic transmission and long-term plasticity in the hippocampus (*1*, *8*), and the mechanisms underlying these developmental changes remain unknown. This uncertainty is attributable, in part, to difficulties in recording from individual pairs of synaptically connected hippocampal neurons; most studies have relied on recordings from populations of pre- and postsynaptic cells (*1*, *8*).

We have now used two approaches that permit the routine recording of synaptic transmission between single CA3 and CA1 pyramidal neurons in hippocampal slices: (i) dual whole-cell patch clamp recording (Fig. 1A) (*9*, *10*); and (ii) focal stimulation of a single presynaptic neuron, by pressing an extracellular stimulating patch pipette onto an individual CA3 cell body (*11*, *12*), and whole-cell recording from a postsynaptic CA1 neuron. Both methods resulted in identical postsynaptic responses (*13*). However, most experiments (24 of 36) were performed with extracellular stimulation because of the difficulty in obtaining stable dual whole-cell recordings.

A given CA1 neuron received functional synaptic input from ~5% of the CA3 neurons tested (Fig. 1A) (*14*). In a synaptically connected pair of neurons from a 6-day-old rat, most CA3 action potentials elicited an excitatory postsynaptic current (EPSC) of ~ −4 pA in a CA1 cell (Fig. 1B). Some stimuli failed to elicit an EPSC. A frequency histogram of EPSC amplitudes showed two prominent peaks that were fitted by the sum of two Gaussian functions (Fig. 1C). One peak, centered at 0 pA with a standard deviation identical to that of the background noise, reflected failures of transmission. The second peak, centered at ~−4 pA, contained most events and reflected successes of transmission. There were no additional peaks at higher current levels. In synapses from young animals (4 to 8 days old), the fraction of successes was consistently high and averaged 0.9 (*13*). In comparison, in slices from older rats (13 to 23 days old), the fraction of successes was significantly lower (<0.5) (Fig. 1, D to F) in agreement with previous, less direct results (*15*). In other respects, however, transmission in older rats resembled that in younger rats: The EPSC amplitude histogram showed only two peaks, one at 0 pA and one at ~−4 pA (Fig. 1, D and E).

The simplest interpretation of these results, based on the classical quantal theory of Katz (*16*), is that a given CA3 neuron makes only a single synaptic contact with a given CA1 neuron. At this contact, a presynaptic action potential either fails to release transmitter or evokes an EPSC that

Center for Neurobiology and Behavior, Department of Pharmacology, and Howard Hughes Medical Institute, College of Physicians and Surgeons, Columbia University, 722 West 168th Street, New York, NY 10032, USA.

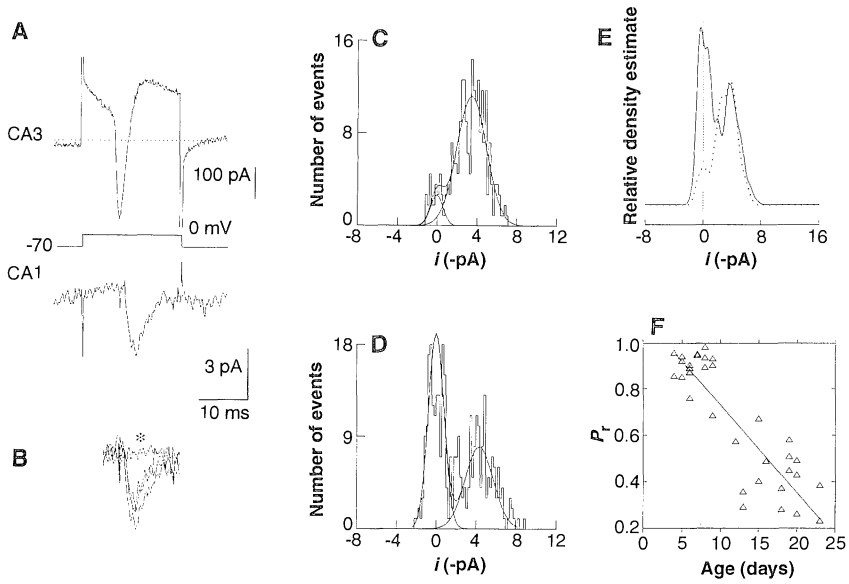

Fig. 1. Recordings from single CA3-CA1 synapses. (**A**) Dual whole-cell recording from a 6-day-old rat. (**Top**) Current in the CA3 neuron during a voltage step to 0 mV from a holding potential of −70 mV. The dotted line shows zero current. (**Bottom**) EPSC recorded simultaneously from the CA1 neuron. (**B**) Several superimposed CA1 EPSCs. Asterisk marks an apparent failure of transmission. (**C**) EPSC amplitude histogram for a 6-day-old rat (255 trials) from the same experiment as in (A) (*i*, current). Solid curve, best-fit sum of two Gaussian functions. The Gaussian fit to the quantal peak showed a mean of −3.48 pA and an SD of 1.48 pA; failure peak, 0 ± 0.63 pA (the failure Gaussian was constrained to be identical to the baseline noise Gaussian). P_r = 0.91. (**D**) EPSC amplitude histogram (327 trials) from a 20-day-old rat. The quantal peak Gaussian showed a mean ± SD of −4.4 ± 1.4 pA; failures peak, 0 ± 0.78 pA. P_r = 0.43. (**E**) Density estimates (9) of the EPSC amplitude distributions obtained from experiments in (C) (dotted line) and (D) (solid line). The density estimate from the 6-day-old rat was scaled so that the quantal peak matched the *y* axis value of the peak from the 20-day-old rat. (**F**) Decrease in P_r during the first 2 to 3 postnatal weeks. Each symbol represents a separate experiment (n = 36). The correlation between P_r and age is significant (r = −0.879, $P < 0.05$). P_r in 4- to 8-day-old and in 13- to 23-day-old rats was 0.89 ± 0.02 (n = 19) and 0.41 ± 0.03 (n = 17), respectively ($P < 0.005$, t test).

represents the response to a single quantum of transmitter (~−4). The probability that a vesicle is released (P_r) is given by the fraction of events under the peak reflecting successes of transmission. Accordingly, the developmental decrease in the fraction of successes represents a progressive decrease in P_r (Fig. 1F). Alternatively, the amplitude of the true quantal event might be too small to resolve, and the peak at ~−4 pA may, in fact, be composed of a number of overlapping unresolved events. The developmental decrease in the fraction of successes could then reflect a decrease in the quantal amplitude, causing us to miss a greater fraction of events. Several lines of evidence presented below, however, suggest that we are indeed accurately measuring the true quantal amplitude and P_r.

One test compared the amplitude distribution of spontaneous miniature EPSCs (mEPSCs) (Fig. 2), which represent quantal responses to the release of single synaptic vesicles (*16*), with that of the evoked EPSCs. The mean amplitude of the mEPSCs was similar to the evoked EPSC quantal amplitude. Furthermore, the mEPSC amplitude distribution did not change during development (Fig. 2C). The coefficient of variation (CV, SD/mean) of the mEPSC distribution was greater than the CV of the quantal peak in the evoked EPSC histogram (Fig. 2D). This result is the opposite of what would be expected if the evoked peak were composed of many unresolved quantal events, which should spread out the distribution and increase the CV. The greater CV of the mEPSCs most likely reflects the fact that these events arise from diverse inputs that may have different quantal amplitudes.

According to quantal analysis at the neuromuscular junction (*16*), failures of transmission are due to failures of release. In contrast, in the central nervous system, such failures have been suggested to reflect failures of postsynaptic reception (*17–20*). According to this view, an entire cluster of postsynaptic receptors in a dendritic spine could be turned on (yielding a success) or off (yielding a failure). However, we have now demonstrated that two interventions known to increase release clearly reduced the number of failures, indicating that they are presynaptic in origin.

We first examined the effects of paired-pulse facilitation (PPF), a widely accepted index of presynaptic function (*21*) (Fig. 3). When two presynaptic stimuli were delivered 50 to 300 ms apart, the average response to the second stimulus was greatly facilitated in 2- to 3-week-old animals (Fig. 3A). The EPSC amplitude histograms showed a marked decrease in the fraction of failures during the second pulse (Fig. 3, B and C), which ranged from 0.5 to 0.1 (n = 3), providing an upper limit for the failures that could be postsynaptic. There was no change in the quantal amplitude or CV of the quantal peak of the second EPSC (*22*), supporting the view that the peak of successes of transmission reflects a single quantal response and that PPF results from an increase in P_r. In contrast to the

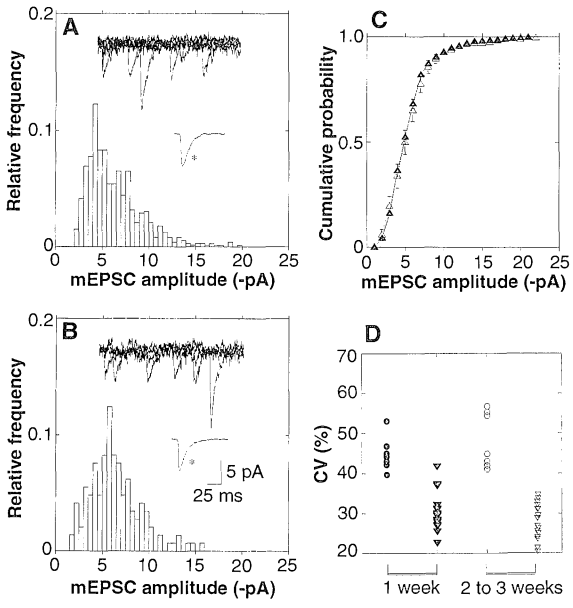

Fig. 2. Comparison between spontaneous mEPSCs and evoked EPSCs from neonatal and 2- to 3-week-old rats. (**A**) Superimposed examples of mEPSCs in a CA1 neuron from a 7-day-old rat (top) and amplitude distribution of mEPSCs from the same cell (mean amplitude, −6.33 ± 0.11 pA; 718 events). Asterisk, average of 100 successive events. (**B**) Amplitude distribution of mEPSCs recorded from a 21-day-old rat (mean amplitude, −6.47 ± 0.22 pA; n = 145). Calibration is the same for (A) and (B). (**C**) Cumulative average amplitude histograms of mEPSCs from 1-week-old rats (filled symbols) (mean amplitude, −6.38 ± 0.21 pA; seven cells) and from 2- to 3-week-old rats (open symbols) (mean, −6.06 ± 0.33 pA; seven cells). (**D**) CV of the evoked unitary EPSCs (triangles) and spontaneous mEPSCs (circles). The CV of mEPSCs and unitary EPSCs in 1-week-old animals was 44.84 ± 1.61% (n = 7) and 30.4 ± 1.01% (n = 19), respectively. In 2- to 3-week-old animals, the CV of mEPSCs and evoked EPSCs was 48.1 ± 2.63% (n = 7) and 28.09 ± 1.04% (n = 19), respectively.

results in 2- to 3-week-old rats, PPF was absent in 4- to 8-day-old animals (Fig. 3, D to F) (*23*), consistent with the observation that P_r is already close to 1 during the first stimulus. The depression during the second pulse may correspond to a transient depletion of docked synaptic vesicles (*24*).

A second line of evidence that the failures were presynaptic was provided by experiments in which release was enhanced by increasing the external Ca^{2+} concentration ($[Ca^{2+}]_0$) under conditions that prevented changes in postsynaptic internal Ca^{2+} (Fig. 4) (*25*, *26*). For 2- to 3-week-old animals, an increase in $[Ca^{2+}]_0$ increased the averaged EPSC by markedly decreasing the fraction of failures (to <0.1) with no change in quantal amplitude or CV (*26*) (Fig. 4, A and B), further limiting the possible fraction of postsynaptic failures and strengthening the view that the quantal peak represents unitary responses. This result also indicated that the failures were not due to failures of the CA3 action potential to invade the presynaptic terminal because high $[Ca^{2+}]_0$ should increase the threshold. In 4- to 8-day-old rats, increasing $[Ca^{2+}]_0$ had no effect on the averaged EPSC, P_r, or quantal amplitude (Fig. 4, C and D) (*26*), consistent with our observation that P_r was normally close to 1.

If LTP results from an increase in release probability (*1*), then the lack of LTP in neonatal rats could be explained by the fact that P_r is nearly maximal. Consistent with this view, the ability to induce LTP was correlated with the developmental decrease in P_r. Moreover, EPSC amplitude histograms showed that LTP, during the 30-min time course of our recordings, was due to an increase in P_r (Fig. 5). There were no changes in quantal amplitude, CV, or shape of the quantal peak distribution (Fig. 5, A and C) (Kolmogorov-Smirnov test, $P > 0.9$), making it unlikely that LTP at this stage results from a postsynaptic change or addition of new functional synapses.

To determine whether the high P_r is indeed responsible for the lack of LTP in 4- to 8-day-old rats, we investigated whether LTP could be expressed in neonatal slices when P_r was reduced by decreasing $[Ca^{2+}]_0$ and increasing $[Mg^{2+}]_0$. External field stimulation of the Schaffer collateral pathway was used to excite multiple CA3 inputs to the CA1 neuron. To induce LTP, we switched from the low $[Ca^{2+}]_0$, high $[Mg^{2+}]_0$ solution to our normal external solution, because of the importance of postsynaptic Ca^{2+} influx for the induction of LTP (*1*). Although the LTP-induction protocol had no effect on the EPSC recorded in normal external solution, on return to the low $[Ca^{2+}]_0$, high $[Mg^{2+}]_0$ solution a persistent potentiation of the EPSC was revealed. This potentiation was not observed when we omitted the LTP-induction protocol ($n = 4$; $t = 0.63$, paired t test) or when the LTP protocol was delivered in the presence of 50 μM D-2-amino-5-phosphonovaleric acid (APV) to block *N*-methyl-D-aspartate (NMDA) receptors (Fig. 5D).

Our results show that the EPSC recorded from a CA1 neuron in response to stimulation of a single presynaptic CA3 neuron was composed of a single quantal event, indicating that a CA3 neuron usually forms a single functional synapse with a given CA1 neuron. This observation is consistent with results obtained by minimal stimulation (*27*, *28*) and anatomic studies suggesting that most CA3 neurons form at most a single contact with a CA1 neuron (*29*). The quantal response may indicate that a presynaptic bouton releases only a single synaptic vesicle per action

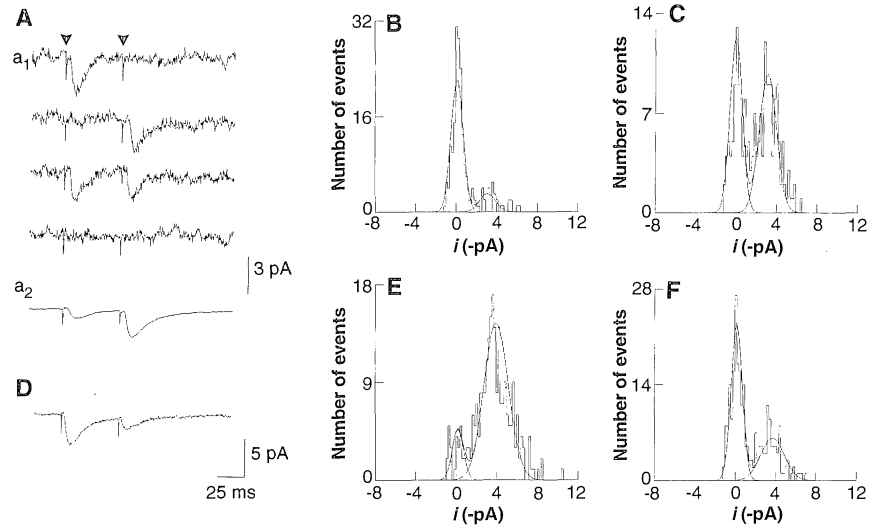

Fig. 3. Comparison of PPF in neonatal and 2- to 3-week-old rats. (**A**) EPSCs recorded from a 19-day-old rat in response to paired stimuli (focal stimulation) with a 50-ms interstimulus interval (a_1), and averaged paired responses from the same experiment, including apparent failures (a_2). Arrowheads indicate time of stimuli. (**B** and **C**) EPSC amplitude histograms for first (B) and second (C) paired responses (197 sweeps). Same experiment as in (A). For (B), $P_r = 0.15$ and quantal amplitude = -3.16 ± 0.79 pA. For (C), $P_r = 0.53$ and quantal amplitude = -3.2 ± 0.85 pA. (**D** to **F**) Same experiment with a 6-day-old rat. (D) Averaged paired responses [same protocol as in (A)]. (E and F) EPSC amplitude distribution of first (E) and second (F) responses ($n = 249$). For (E), $P_r = 0.87$ and quantal amplitude = -4.01 ± 1.2 pA. For (F), $P_r = 0.36$ and quantal amplitude = -3.76 ± 1.16 pA.

Fig. 4. Effect of an increase in $[Ca^{2+}]_0$ on EPSCs. (**A**) EPSC amplitude histogram for an 18-day-old rat at normal (2.5 mM) $[Ca^{2+}]_0$ (300 trials). (**Inset**) Superimposed successive EPSCs (focal stimulation). $P_r = 0.37$. (**B**) EPSC amplitude histogram for the same neuron as in (A) at increased (5.0 mM) $[Ca^{2+}]_0$ (537 trials). $P_r = 0.84$. (**C**) EPSC amplitude distribution for a 5-day-old rat at normal $[Ca^{2+}]_0$ (300 sweeps). $P_r = 0.94$. (**D**) EPSC amplitude histogram for the same neurons in (C) at increased (5.0 mM) $[Ca^{2+}]_0$ ($n = 338$). $P_r = 0.97$ (focal stimulation) (*26*).

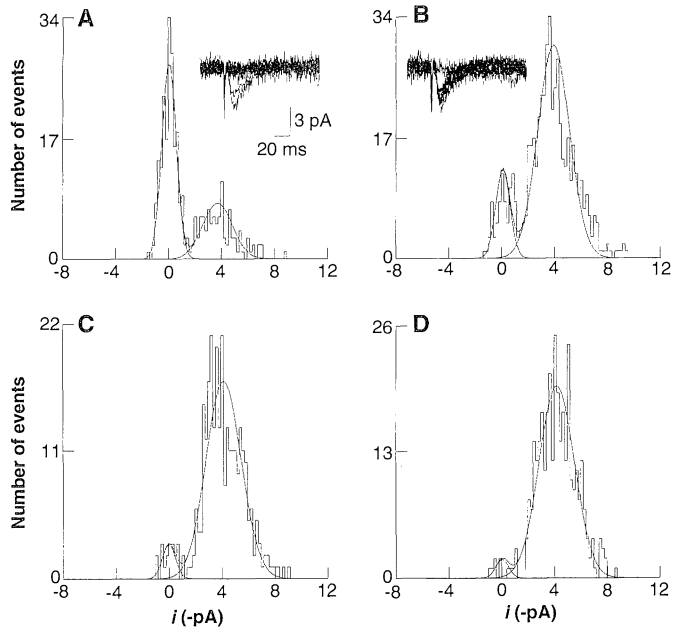

potential, or that the transmitter content of a single vesicle is sufficient to saturate the postsynaptic receptors (*27*). Failures of transmission at this synapse appear to reflect presynaptic failures to release transmitter (*16*) rather than silent clusters of postsynaptic receptors (*17–20*). Paired recordings at a synapse from CA3 pyramidal neurons onto inhibitory interneurons also reveal only a single release site (*30*). In contrast, dentate gyrus granule neurons (*11*) and inhibitory interneurons (*31*) evoke multiquantal responses in their hippocampal targets, suggesting that the number of synaptic contacts may depend on the identity of the presynaptic neuron and not on the identity of its target.

The observation that LTP is due to an increase in P_r, with little change in quantal amplitude, agrees with data on mEPSCs in cultured neurons (*32*), a study in which minimal stimulation was used to excite single CA3 axons (*33*), and recent data showing a change in synaptic vesicle turnover (*34*). In contrast, other studies based on mEPSC analysis (*35*) and minimal stimulation (*36*) have shown an increase in quantal amplitude. A failure to detect changes in quantal amplitude may be due to the fact that our measurements were limited to the first 30 min after LTP induction (*37*). Our results differ from a recent study with minimal stimulation that concluded that LTP results from the unmasking of silent clusters of non-NMDA glutamate receptors (*20*).

The high P_r in the hippocampus of 4- to 8-day-old animals can explain why PPF and LTP are absent, and why LTD, which is associated with a persistent decrease in P_r (*7, 33*), is pronounced at this stage. Other regions of rat brain, including visual cortex and somatosensory cortex, undergo an opposite developmental regulation, in which LTP disappears 1 week after birth (*38*). Thus, synaptic plasticity in the brain is not a fixed property but is differentially regulated in separate areas, presumably to subserve distinct developmental and memory-related functions.

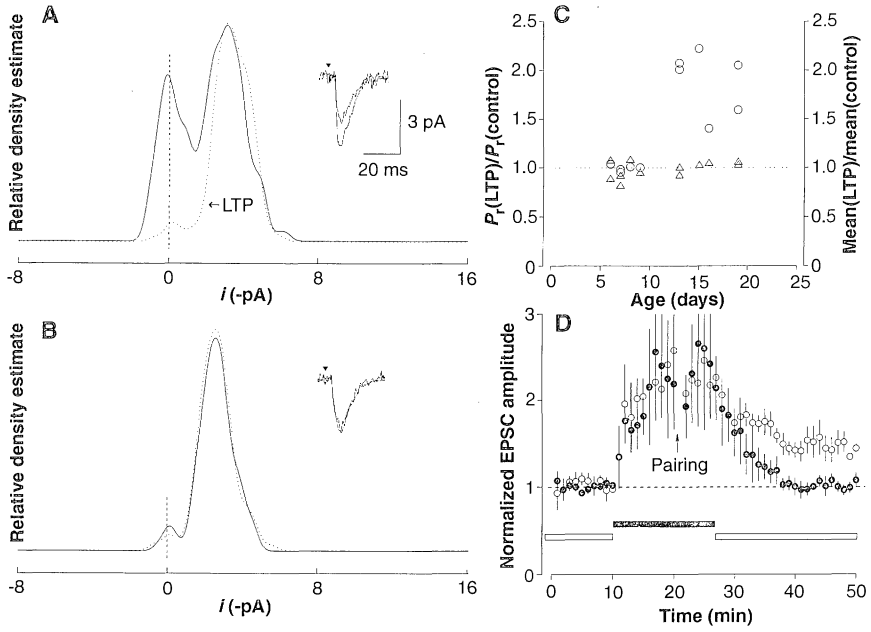

Fig. 5. Developmental changes and presynaptic expression of LTP. (**A**) Density estimates of EPSCs before (176 sweeps, solid line) and after (400 sweeps, dotted line) induction of LTP in a slice from a 19-day-old rat. Density estimates were scaled so that quantal peak *y* axis values matched. For induction of LTP, the CA1 neuron was held at +10 mV and 60 presynaptic action potentials were evoked at 2 Hz. (**Inset**) Averaged postsynaptic response (including apparent failures) before and after LTP. Arrowhead indicates time of stimulus. Control: P_r = 0.58, quantal amplitude = −3.56 ± 1.03 pA. After LTP: P_r = 0.92, quantal amplitude = −3.65 ± 0.94 pA. (**B**) Similar experiment for a 6-day-old rat. Solid line, before LTP (110 events); dotted lines, after LTP (381 events). (**Inset**) Averaged EPSC (including failures) before and after LTP. Control: P_r = 0.90, quantal amplitude = −3.04 ± 0.86 pA. After LTP: P_r = 0.93, quantal amplitude = −2.9 ± 0.85 pA. (**C**) Summary of all LTP experiments with animals of different ages. P_r (○) and quantal amplitudes (△) calculated for all events after LTP were normalized by their values before LTP and plotted as a function of the age of the animal. (**D**) Unmasking of LTP in 4- to 8-day-old animals. Compound EPSCs were elicited by field stimulation of the Schaffer collateral pathway with bipolar electrodes in low $[Ca^{2+}]_o$ (1.0 mM), high $[Mg^{2+}]_o$ (2.5 mM) solution (open bar) or normal external solution (2.5 mM Ca^{2+}, 1.0 mM Mg^{2+}) (filled bar). Switching to normal solution enhanced the EPSC as a result of the effect of $[Ca^{2+}]_o$ on P_r. LTP-induction protocol (pairing) was applied at the arrow. (○) No APV (n = 5); (●) 50 μM APV (n = 4). Error bars indicate SEM.

REFERENCES AND NOTES

1. T. V. P. Bliss and G. L. Collingridge, *Nature* **361**, 31 (1993).
2. R. C. Malenka, *Proc. Natl. Acad. Sci. U.S.A.* **90**, 3121 (1993); D. Linden and J. A. Connor, *Annu. Rev. Neurosci.* **18**, 319 (1995).
3. M. Constantine-Paton, H. T. Cline, E. Debski, *Annu. Rev. Neurosci.* **13**, 1229 (1990); T. M. Jessell and E. R. Kandel, *Neuron* **10**, 1 (1993).
4. D. Purves and J. W. Lichtman, *Principles of Neural Development* (Sinauer, Sunderland, MA, 1985).
5. M. Baudry, D. Arst, M. Oliver, G. Lynch, *Dev. Brain Res.* **1**, 37 (1981).
6. S. M. Dudek and M. F. Bear, *J. Neurosci.* **13**, 2910 (1993).
7. V. Y. Bolshakov and S. A. Siegelbaum, *Science* **264**, 1148 (1994).
8. H. Korn and D. S. Faber, *Trends Neurosci.* **14**, 439 (1991).
9. R. Malinow, *Science* **252**, 722 (1991).
10. Hippocampal slices (250 to 300 μm) were prepared from 4- to 23-day-old Sprague-Dawley rats (*7*) and superfused with a solution that contained 119 mM NaCl, 2.5 mM KCl, 2.5 mM $CaCl_2$, 1.0 mM $MgSO_4$, 1.0 mM NaH_2PO_4, 26.2 mM $NaHCO_3$, 10 mM glucose, and 100 μM picrotoxin and was equilibrated with 95% O_2 and 5% CO_2 (pH 7.3 to 7.4) at 21° to 23°C. Whole-cell recordings [M. G. Blanton, J. J. Lo Turco, A. R. J. Kriegstein, *J. Neurosci. Methods* **30**, 203 (1989)] were obtained either from CA1 or simultaneously from CA3 and CA1 pyramidal cells. The patch electrodes (5 to 10 megohms) contained 130 mM cesium gluconate, 0.4 mM $CaCl_2$, 1.1 mM EGTA, 5.0 mM NaCl, 1.0 mM $MgCl_2$, 10 mM Hepes (pH 7.2), 2.0 mM adenosine triphosphate (Mg^{2+} salt), and 0.1 mM guanosine triphosphate (Na^+ salt). Occasionally, 130 mM KCl was used with similar results. Series resistance ranged from 15 to 30 megohms and was constant during the experiment and identical for rats of all ages. The excitatory postsynaptic currents (EPSCs) were filtered at 1 to 2 kHz and digitized at 2.5 to 5 kHz. The EPSC amplitudes were measured as the difference between the mean current during a prestimulus baseline and the mean current over a 1- to 2-ms window at the peak of the response. Noise was measured by placing the same window at the baseline before the stimulus. EPSC amplitude density estimates were constructed with software provided by R. Malinow (*9*). A single Gaussian distribution was fitted to the binned baseline noise histogram obtained from current values recorded immediately before the stimulus. The evoked distributions were then fitted by the sum of two Gaussian functions, one of which was constrained so that its mean and SD equaled the baseline noise values. The mean, SD, and relative area of the success peak were all free parameters in the nonlinear least squares fit (Simplex routine). The probability of transmitter release (P_r) was measured from the fractional area under the Gaussian peak corresponding to successes. The mean and SD for the success peak from the Gaussian fits were within 10% of the values calculated directly from events judged to be successes, indicating that the Gaussian fits provide a reasonable and objective description of the data. Holding potential of the CA1 neuron was −70 mV. Miniature EPSCs were recorded in the presence of 1 μM tetrodotoxin, 200 mM sucrose, and 100 μM picrotoxin and analyzed as described (*7*).
11. P. Jonas, G. Major, B. Sakmann, *J. Physiol. (London)* **472**, 615 (1993).
12. The EPSCs were evoked by low-intensity current pulses (50 to 100 μA, 50- to 100-μs duration) applied through a fine-tipped (2 μm), silver-painted patch pipette pressed onto the CA3 cell body layer. The mean EPSC amplitude showed a steep all-or-none threshold as a function of current intensity. Increasing current intensity 100% above this threshold had no effect on the EPSC, indicating stimulation of a single presynaptic input.
13. The P_r at synapses from 4- to 8-day-old rats was 0.90 ± 0.02 (n = 9) from dual whole-cell recordings and 0.89 ± 0.03 (n = 10) from focal stimulation (no significant difference, t test; t = 0.37). The P_r at

synapses from 13- to 23-day-old rats was 0.50 ± 0.07 (n = 3) from dual whole-cell recording and 0.39 ± 0.04 (n = 14) from focal stimulation (no significant difference, t = 1.36).
14. R. J. Sayer, M. J. Friedlander, S. J. Redman, *J. Neurosci.* **10**, 826 (1990).
15. C. Rosenmund, J. D. Clements, G. L. Westbrook, *Science* **262**, 754 (1993); N. A. Hessler, A. M. Shirker, R. Malinow, *Nature* **366**, 569 (1993).
16. B. Katz, *The Release of Neural Transmitter Substances* (Liverpool Univ. Press, Liverpool, UK, 1969).
17. F. Edwards, *Nature* **350**, 271 (1991).
18. D. M. Kullman, *Neuron* **12**, 1111 (1994).
19. R. Malinow, *Science* **266**, 1195 (1994).
20. D. Liao, N. A. Hessler, R. Malinow, *Nature* **375**, 400 (1995).
21. R. S. Zucker, *Annu. Rev. Neurosci.* **12**, 13 (1989).
22. Averaged values of quantal parameters for PPF in 1-week-old animals: First EPSC, P_r = 0.93 ± 0.03, quantal amplitude = −4.29 ± 0.18 pA, CV of quantal peak = 30.21 ± 0.48%; second EPSC, P_r = 0.21 ± 0.08 [significantly different from first EPSC (t = 6.38, $P < 0.005$; paired t test], quantal amplitude = − 4.16 ± 0.25 pA [no significant difference (t = 1.82)], CV = 28.86 ± 1.0% [no significant difference (t = 1.25)]. Averaged values for 2- to 3-week-old animals: First EPSC, P_r = 0.21 ± 0.03, quantal amplitude = − 3.33 ± 0.15 pA, CV of quantal peak = 30.35 ± 2.82%; second EPSC, P_r = 0.66 ± 0.11 (t = 5.418, $P < 0.005$), quantal amplitude = −3.26 ± 0.2 pA [no significant difference (t = 0.78)], CV = 29.8 ± 1.62% [no significant difference (t = 0.41)]. For all experiments, n = 3.
23. D. Muller, M. Oliver, G. Lynch, *Dev. Brain Res.* **49**, 105 (1989).
24. C. F. Stevens and T. Tsujimoto, *Proc. Natl. Acad. Sci. U.S.A.* **92**, 846 (1995).
25. F. A. Dodge and R. A. Rahamimoff, *J. Physiol. (London)* **193**, 419 (1967); R. A. Mallart and A. R. Martin, *ibid.* **196**, 593 (1968); J. E. Zengel and K. L. Magleby, *J. Gen. Physiol.* **76**, 175 (1980).
26. *N*-Methyl-D-aspartate receptors were blocked with D-2-amino-5-phosphonovaleric acid (50 μM), and the CA1 cell was dialyzed with 10 mM BAPTA [1,2-bis(2-aminophenoxy)ethane-*N,N,N′,N′*-tetraacetic acid] to eliminate changes in CA1 cell internal Ca^{2+} in response to increasing $[Ca^{2+}]_o$. Gaussian fits to quantal peaks were as follows: Fig. 4A, −3.79 ± 1.12 pA; Fig. 4B, −4.0 ± 1.2 pA; Fig. 4C, −4.2 ± 1.32 pA; and Fig. 4D, −4.2 ± 1.3 pA (means ± SD). Averaged values of release parameters for 4- to 8-day-old animals were as follows: Normal $[Ca^{2+}]_o$, P_r = 0.89 ± 0.03, quantal amplitude = −4.14 ± 0.07 pA, CV of quantal peak = 32.8 ± 2.18%, mean EPSC = −3.98 ± 0.16 pA; increased $[Ca^{2+}]_o$, P_r = 0.93 ± 0.02 [no significant difference from value in normal Ca^{2+} (t = 1.19, paired t test)], quantal amplitude = −4.19 ± 0.041 pA [no significant difference (t = 1.64)], CV = 34.1 ± 1.02% [no significant difference (t = 0.53)], mean EPSC = −4.3 ± 0.1 pA [no significant difference (t = 2.42)]. Averaged values for 2- to 3-week-old rats were as follows: Normal $[Ca^{2+}]_o$, P_r = 0.42 ± 0.04, quantal amplitude = −4.4 ± 0.34 pA, CV = 29.96 ± 2.16%, mean EPSC = −1.86 ± 0.4 pA; increased $[Ca^{2+}]_o$, P_r = 0.86 ± 0.02 [significantly different from value in normal Ca^{2+} ($P < 0.005$, paired t test)], quantal amplitude = −4.35 ± 0.19 pA [no significant difference (t = 2.13)], CV = 27.7 ± 1.2% [no significant difference (t = 1.01)], mean EPSC = −3.94 ± 0.24 pA [significant difference ($P < 0.01$)]. For all averages, n = 3.
27. M. Raastad, J. F. Storm, P. Andersen, *Eur. J. Neurosci.* **4**, 113 (1992).
28. C. F. Stevens and Y. Wang, *Neuron* **14**, 795 (1995).
29. K. E. Sorra and K. M. Harris, *J. Neurosci.* **13**, 3736 (1993). A minority of axons appeared to make multiple contacts with a CA1 neuron at the light-microscopic level; in some instances, a single presynaptic bouton contacted two postsynaptic spines.
30. A. J. Gulyas, R. Miles, A. Sik, K. Toth, N. Tamamaka, *Nature* **366**, 683 (1993); O. Arancio, H. Korn, A. Gulyas, T. Freund, R. Miles, *J. Physiol. (London)* **481**, 395 (1994).
31. F. A. Edwards, A. Konnerth, B. Sakmann, *J. Physiol. (London)* **430**, 213 (1990).
32. A. Malgaroli and R. W. Tsien, *Nature* **357**, 134 (1992).
33. C. F. Stevens and Y. Wang, *ibid.* **371**, 704 (1994).
34. A. Malgaroli *et al.*, *Science* **268**, 1624 (1995).
35. T. Manabe, P. Renner, R. A. Nicoll, *Nature* **355**, 50 (1992).
36. D. M. Kullmann and R. A. Nicoll, *ibid.* **357**, 240 (1992); D. Liao, A. Jones, R. Malinow, *Neuron* **9**, 1089 (1992); A. Larkman, T. Hannay, K. Stratford, J. Jack, *Nature* **360**, 70 (1992).
37. S. N. Davies, R. A. J. Lester, K. G. Reymann, G. L. Collingridge, *Nature* **338**, 500 (1989).
38. M. C. Crair and R. C. Malenka, *ibid.* **375**, 325 (1995); A. Kirkwood, H.-K. Lee, M. F. Bear, *ibid.*, p. 328.
39. We thank B. Armitage, R. Hawkins, and E. Kandel for their helpful comments on the manuscript, and R. Malinow for providing computer software for calculation of density estimates.

4 April 1995; accepted 11 July 1995

Regulated Subcellular Distribution of the NR1 Subunit of the NMDA Receptor

Michael D. Ehlers, Whittemore G. Tingley, Richard L. Huganir*

NMDA (*N*-methyl-D-aspartate) receptors are selectively localized at the postsynaptic membrane of excitatory synapses in the mammalian brain. The molecular mechanisms underlying this localization were investigated by expressing the NR1 subunit of the NMDA receptor in fibroblasts. NR1 splice variants containing the first COOH-terminal exon cassette (NR1A and NR1D) were located in discrete, receptor-rich domains associated with the plasma membrane. NR1 splice variants lacking this exon cassette (NR1C and NR1E) were distributed throughout the cell, with large amounts of NR1 protein present in the cell interior. Insertion of this exon cassette into the COOH-terminus of the GluR1 AMPA (α-amino-3-hydroxy-5-methyl-4-isoxazole propionate) receptor was sufficient to cause GluR1 to be localized to discrete, receptor-rich domains. Furthermore, protein kinase C phosphorylation of specific serines within this exon disrupted the receptor-rich domains. These results demonstrate that amino acid sequences contained within the NR1 molecule serve to localize this receptor subunit to discrete membrane domains in a manner that is regulated by alternative splicing and protein phosphorylation.

Aggregation of neurotransmitter receptors in the postsynaptic membrane is a process crucial for synaptogenesis. Like acetylcholine receptors (AChRs) at the neuromuscular junction (*1*), neurotransmitter receptors in the central nervous system (CNS) are localized at postsynaptic sites (*2*–*6*), although the mechanisms involved are less well understood. The NMDA class of glutamate receptors plays a critical role in synaptic plasticity, synaptogenesis, and excitotoxicity (*7*). Iontophoretic mapping and immunoelectron microscopy reveal that NMDA receptors are concentrated at synaptic sites (*4, 5*). Moreover, actin filament stabilization prevents Ca^{2+}-induced rundown of NMDA current (*8*), and NMDA responses are sensitive to cytoskeletal strain (*9*), suggesting a cytoskeletal association of the NMDA receptor.

NMDA receptors consist of two families of homologous subunits (NR1 and NR2A-D) (*10, 11*). The NR1 subunit is able to form functional homomeric channels (*10*), which may be present in vivo (*12, 13*). Expression of NR2 subunits with the NR1 subunit, however, increases NMDA receptor current, and most NMDA receptors in the brain are thought to be heteromeric complexes of NR1 and NR2 subunits (*11, 14*). At least seven NR1 splice variants (NR1A-G) are expressed in the brain (*13, 15, 16*) that differ in their spatial and temporal expression patterns (*17*), in their sensitivity to polyamines, phorbol esters, and Zn^{2+} (*13, 16*), and in their ability to be phosphorylated by protein kinase C (PKC) (*18*).

To examine the mechanism of subcellular targeting of the NR1 subunit, we transfected QT6 quail fibroblasts (*19*) with the complementary DNA (cDNA) encoding the NR1A subunit and examined them by immunofluorescent microscopy (*20, 21*). The QT6 cell line has been used as a model system for studying AChR clustering induced by the synaptic protein 43K (*22*). Immunofluorescent staining revealed the presence of highly concentrated regions of NR1A protein (Fig. 1A). These NR1-enriched domains manifested themselves as patches or elongated stripes as well as punctate microclusters. The organization of NR1 into highly concentrated domains is unique among heterologously expressed glutamate receptors we have examined. For example, the AMPA receptor subunit GluR1 and the kainate receptor subunit GluR6 are found throughout transfected QT6 cells, with large amounts of intracellular staining and no regions of receptor enrichment (Fig. 1, B and C). Indeed, within the same cell cotransfected with both GluR1

Department of Neuroscience, Howard Hughes Medical Institute, Johns Hopkins University School of Medicine, Baltimore, MD 21205, USA.

*To whom correspondence should be addressed.